RAA 2017 Vol. **17** No. **12**, 124 (12pp) doi: 10.1088/1674–4527/17/12/124

http://www.raa-journal.org *http://iopscience.iop.org/raa*

Research in Astronomy and Astrophysics

Preliminary study on broadband antireflection coatings for large aperture telescopes

Ye-Ru Wang[1,2,3], Xin-Nan Li[1,2], Jin-Feng Wang[1,2] and Jie Tian[1,2]

[1] National Astronomical Observatories/Nanjing Institute of Astronomical Optics & Technology, Chinese Academy of Sciences, Nanjing 210042, China; *yrwang@niaot.ac.cn*

[2] Key Laboratory of Astronomical Optics & Technology, Nanjing Institute of Astronomical Optics & Technology, Chinese Academy of Sciences, Nanjing 210042, China

[3] University of Chinese Academy of Sciences, Beijing 100049, China

Received 2017 May 10; accepted 2017 August 29

Abstract A broadband anti-reflective (AR) coating design for astronomical large-aperture telescopes is proposed. We give simulations of two-, three- and four-layer silica sol-gel on fused silica and finally get the optimal optical constants. As a comparison, we discuss the traditional dielectric material that has been applied to broadband AR coatings. To better guide the following experiment, we also conduct error analysis and feasibility analysis, combining with the technological characteristics of sol-gel. The analytical method is suitable for other wavebands and substrates. It is also instructive for large area AR coatings in the field of solar cells.

Key words: instrumentation: miscellaneous — methods: numerical — techniques: spectroscopic

1 INTRODUCTION

It is more and more difficult to apply appropriate anti-reflective (AR) coatings onto transmission optical elements, the apertures of which are gradually increasing as large ground-based optical/infrared telescopes develop (Tokunaga 2014). Despite the fact that most large-scale telescopes adopt segmented mirror active optics and reflective optical structures, many large-aperture prisms, which could improve the light gathering power and collect more information from observed objects, are used in terminal equipment such as various spectrographs (Angeli et al. 2004). In addition, the hermetic windows of many telescopes need AR coatings to be applied. Unlike AR coatings that are used in solar cells and other devices which only focus on their transmission properties (Kanamori et al. 2002; Liu et al. 2012), rigorous surface precision is desired for the optical lens in a telescope, especially the correctors. Thus, we hope that the thickness of a coating would be as small as possible and the whole coating growth process could be carried out under lower temperature, which will have less influence on the associated surface precision. In addition, a good spectral reproduction ability is very important, which makes the subsequent spectral analysis more precise and easier. In view of the fact that most dielectric materials absorb in the ultraviolet wavelength region, the limited number of alternative materials in coating design yields an unsatisfactory spectral transmittance when they are applied to telescopes whose working waveband ranges from ultraviolet to near infrared.

At the beginning of this century, sol-gel coatings were firstly applied in large-aperture telescopes and an encouraging ultra-broadband AR result was achieved (Phillips et al. 2008). The Atmospheric Dispersion Corrector (ADC) for the Keck-I Cassegrain focus with fused silica prisms is about 1022 mm in diameter. This is a simple structure of silica sol-gel over an MgF_2 layer, which was conventionally obtained by vacuum deposition, producing a well-formed coating from 310 nm to 1100 nm (Phillips et al. 2006). The relatively-low refractive index (RI) of silica sol-gel is perfectly matched with the fused prisms, and there is a smaller RI difference between the silica sol-gel and incident medium (i.e. air). The features above make it possible to achieve a good broadband transmittance with only two layers. On the contrary, many more layers should be applied if tradi-

tional dielectric materials are used. Therefore, we reduce the thickness and number of layers by employing sol-gel coatings, and moreover, the transmittance results become even better. In addition, the sol-gel process has many advantages compared to traditional vacuum dielectric films, such as a minor restriction in the substrate shape and size, better homogeneity, simple techniques and processing at a lower temperature. There are many larger optics in the Thirty Meter Telescope (TMT), which is under construction, and in the Large Optical/Infrared Telescope (LOT), which is planned in China (Zhang et al. 2016). Problems that exist in the process of dielectric film deposition, such as material limitations in ultraviolet region, film uniformity and process safety, would be perfectly eliminated on condition that the dielectric layer is replaced by silica sol-gel. An exciting prospect for applying sol-gel coatings in astronomical telescopes could be possible.

In this paper, this problem will be discussed in detail. We firstly carry out numerical simulations for sol-gel broadband AR coatings, focusing on the coating design, and we also hope to propose an ideal coating structure in theory and finally obtain some good results. These simulations are based on existing experimental facts rather than a theoretical possibility. Then, we conduct feasibility and error analyses combined with specific processes, and finally discard some solutions that are extremely difficult to implement. The results can give some basic guidelines for subsequent experiments.

2 THEORY AND HYPOTHESIS

Reflection and transmission occur when light arrives at the interface of two different media, the RIs of which are n_0 and n_1, respectively (Born & Wolf 1959). The reflectivity of the normal angle of incidence is $R = [(n_0 - n_1)/(n_0 - n_1)]^2$, supposing that the media are nonabsorbent. For common BK-7 glass, the RI of which is about 1.52, the reflectivity is as high as 4% from one side; in other words, the transmittance is only about 92%. An ideal homogeneous single-layer AR coating could achieve zero reflection at the reference wavelength while satisfying the following conditions: the optical thickness of the coating should be $\lambda/4$, where λ is the reference wavelength; and $n_{\rm c} = (n_{\rm a}n_{\rm s})^{1/2}$, where $n_{\rm a}$, $n_{\rm c}$ and $n_{\rm s}$ are the RIs of the air, coating and substrate, respectively. For a dielectric material, in order to achieve near zero reflection of the monolayer, the RI of the substrate, which is calculated under the above conditions, should be at least 1.9, and it is clear that most substrates with a low RI do not satisfy this condition. Due to its loose and porous characteristics, the RI of silica sol-gel is very low, which perfectly matches the low RI substrate, and thus zero reflectance at a special wavelength can be achieved. However, an effective near-zero reflectance is achieved only for a narrow spectral width around the reference wavelength because of the uniform RI throughout the whole coating. In the rest of the waveband, the reflectance will increase rapidly up to the bare substrate at half-wavelength.

Let us go back to the reflectance formula concerning light traveling between two media with different RI, $R = [(n_0 - n_1)/(n_0 - n_1)]^2$. We can draw a conclusion that the smaller the difference in RI between adjacent layers is, the smaller the reflection loss is. It is conceivable that there will be nearly no reflection loss when the RI of the coating changes slowly from the substrate to air, that is to say, a sharp variation of RI between adjacent layers should be avoided. The ideal condition would be that the RI continuously decreases from the bottom to the top of the coating, which is the so-called gradient-index AR coating.

Since the 1960s, a great many of papers have focused on design and application of optical gradient-index coatings (Anders & Eichinger 1965; Southwell 1983, 1985; Dobrowolski et al. 2002). There are many advantages besides perfect broadband and omnidirectional spectral performance, e.g. excellent mechanical properties (Rats et al. 1999), fewer scattering losses (Arnon 1977), less residual stress (Tang et al. 2011), enhanced resistance to laser damage (Ristau et al. 2008) and enhanced temperature stability (Tang et al. 2011). However, it is very difficult to manufacture gradient-index coatings that can be used in optical and infrared bands. Although some special process may be used to produce materials with continuous changes in RI (Li et al. 2010; Huang et al. 2007), the production process is complicated, which is not suitable for large scale fabrication, and the scope of application is limited. A multilayer coating can be viewed as a discrete approximation of the gradient-index AR coating, which is described as a quasi-gradient coating, so a more feasible method is to use several uniform sub-layers to approximate the inhomogeneous gradient-index coating. Until now, the oblique-angle deposition and chemical etch-leach process have been applied to successfully manufacture quasi-gradient coating (Xi et al. 2007; Liu et al. 2012), but they are not suitable for an astronomical lens. Through our analysis, three layers, or even two layers of sol-gel film, achieve excellent broadband AR effect. This method has excellent prospects for application in the field of broadband large-aperture telescopes due to its advantages in film uniformity, low-stress and suitability for large area plating. At the same time, sol-gel coatings can also be applied to the field of solar cells,

so that the photoelectric conversion efficiency could be widely improved.

The sol-gel process is a kind of chemical coating method. The usual practice is to have organic metal alkoxide dissolved in ethanol or methanol and then to add water as a hydrolytic reagent, which is accelerated by catalysts. Here we use tetraethyl orthosilicate as a reactant and the overall reaction is shown as follows (Thomas 1986, 1992)

$$\mathrm{Si(OC_2H_5)_4 + 2H_2O \longrightarrow SiO_2 + 4C_2H_5OH.}$$

We often use concentrated hydrochloric acid or concentrated ammonia as a catalyst, which also supplies the water. According to the various catalysts being added, this reaction will produce products that are different in their microstructures, which would affect the coating properties. With acid catalyzing, a siloxane chain structure with an alkoxy and hydroxyl group is firstly formed. It will be in continuous polycondensation as the solvent evaporates after being coated until a cross-linking, dense SiO_2 coating is formed, which has the characteristics of low porosity and high RI (approximately 1.43). With an alkalinious catalyst, the sol tends to form a monodisperse silica colloidal suspension. By adjusting the process parameters, the silica colloid can be maintained in a size and morphology ($\sim$20 nm) suitable for coating. As a result, the coating is made up of disordered accumulational silica particles with high porosity and low RI. Considering two different RIs composed of acid and base catalyzed suspensions, we add the acid catalyzed sol to the base catalyzed sol in a certain proportion, which is the so-called two-step method. The siloxane chain structure acts as a linking medium for the alkali-catalyzed sol suspended particles, then a material with an RI between them is prepared. The RI adjustment range depends on the two mixed sols (Thomas 1992).

The simplified quasi-gradient form usually follows the theoretical numerical solutions. Considering that the particular coating design depends on the available coating technology, we give the quasi-gradient coating design directly, combined with experimental facts and practical experience. We also give the error and feasibility analysis. To better guide our experiments in the future, we exclude results that are either impossible or difficult to achieve. So, several notes are proposed for better simulation as follows.

(1) Considering that the operating bands of the ADC at KECK and TMT are about 300–1100 nm, our optimization is also within this range.
(2) The alkali-catalyzed thin film silica particles are about 20 nm in diameter. Taking the film thickness uniformity into account, we set the optimized film thickness of a single layer to be at least 50 nm.
(3) Due to the limitation of the RI and difficulty in controlling thickness accuracy, we will give the tolerance range for optical constants and their influence on the transmittance and examine the feasibility of the designed film structure.
(4) Fused silica is chosen as the substrate, which is commonly used and has no absorption in the ultraviolet band.
(5) In the optimized band, the silica sol-gel film is in normal dispersion. In order to better fit its true dispersion curve, the simulation value is set to a linear relationship, as shown in Figure 1. There is a different value of 0.01 in the RI between the center wavelength and the edge of the wavelength band, which is

$$y = -2.5 \times 10^{-5} x + 0.0175 + n_{\mathrm{mid}}\,, \qquad (1)$$

where n_{mid} is the value of the RI at the center of the band (i.e. 700 nm). Of course, you can also ignore the dispersion, which has little effect on spectral performance.

With the assistance of Essential Macleod, we will start our simulations from the simplest two-layer film, to find the best combination of RI and film thickness and finally give the optimum solution. The analysis method can be applied to more layers and the target band can also be changed as needed, but the analysis method remains unchanged.

3 NUMERICAL SIMULATION AND ANALYSIS

By means of the acid-base two-step method, the RI can be continuously adjusted from the alkali-catalyzed film (with n about 1.18) to the acid-catalyzed film (with n of 1.42 or so). Our basic idea is to discretize the RI with the sample interval $\Delta n = 0.03$ and the results are as follows

$$\begin{aligned} n =& 1.43, 1.40, 1.37, 1.34, 1.31, \\ & 1.28, 1.25, 1.22, 1.19, 1.16. \end{aligned}$$

For multilayer coatings, different RI values are assigned to each layer, and then we optimize thickness for each combination, the aim of which is to make the transmittance in each point as high as possible in the target band. The best coating structure would be sought out after comparing the optimal solutions of all RI combinations. Since the transmittance varies continuously with the RI and thickness, i.e., there is no abrupt change, our results could be accordingly considered as the optimal solution with a certain number of layers.

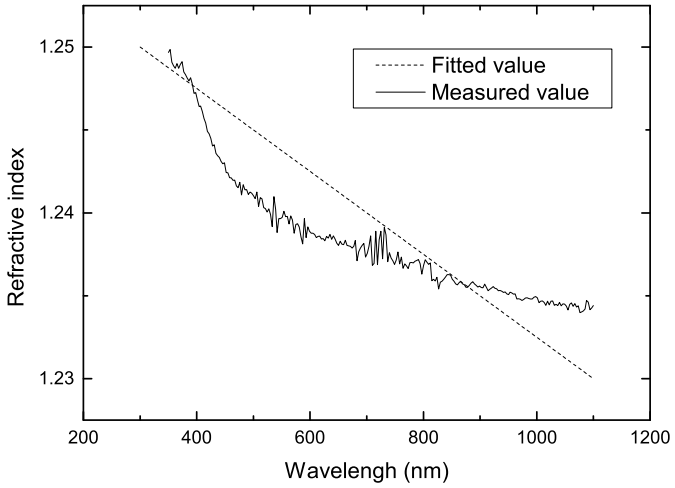

Fig. 1 The *solid* line represents measured data by an ellipsometer, and the *dashed* one is the fitted result.

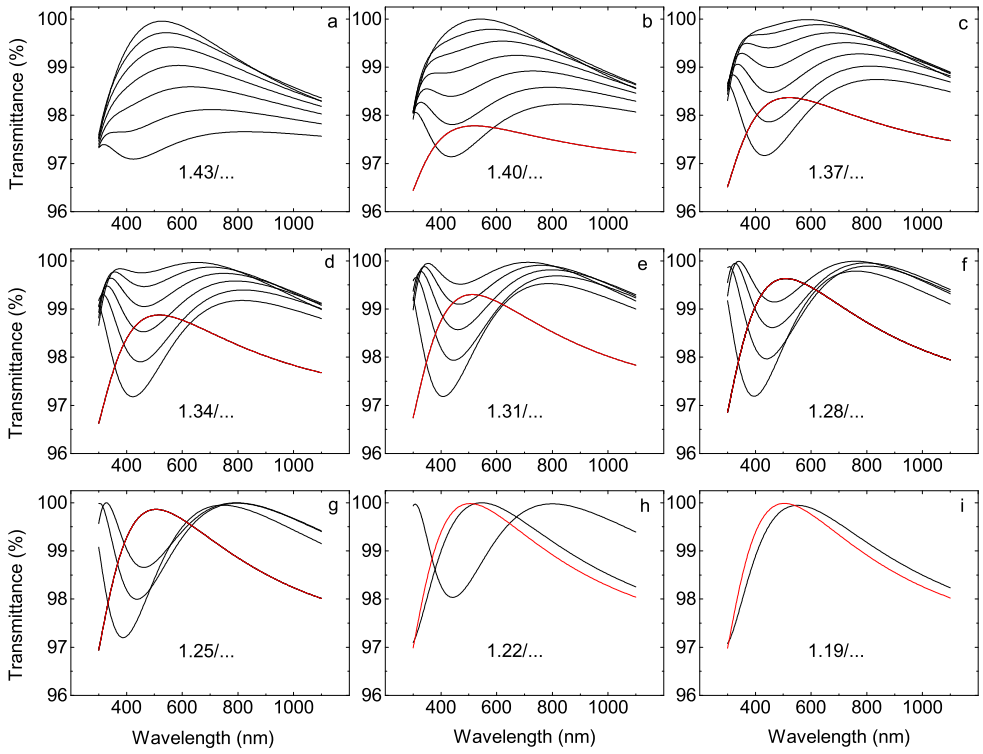

Fig. 2 Transmittance that changes with n_1 when n_2 is fixed. The curves go down with an increase of n_1 in the visible region, and the *red* lines represent conditions in which $n_1 > n_2$.

3.1 Two-layer System

Assuming that the RI of the outer layer is n_1, and the film thickness is d_1, similarly, n_2 and d_2 are the optical constants of the inner layer. By means of the control variable method, n_1 and n_2 are fixed respectively to investigate the impact of RI variation of the other layer on transmittance. The following results, unless particularly stated, are for single-sided transmittance.

Firstly, the RI of the inner layer is fixed, the structure of which is Sub/n_2/$\cdots$/Air. The transmittance curves are

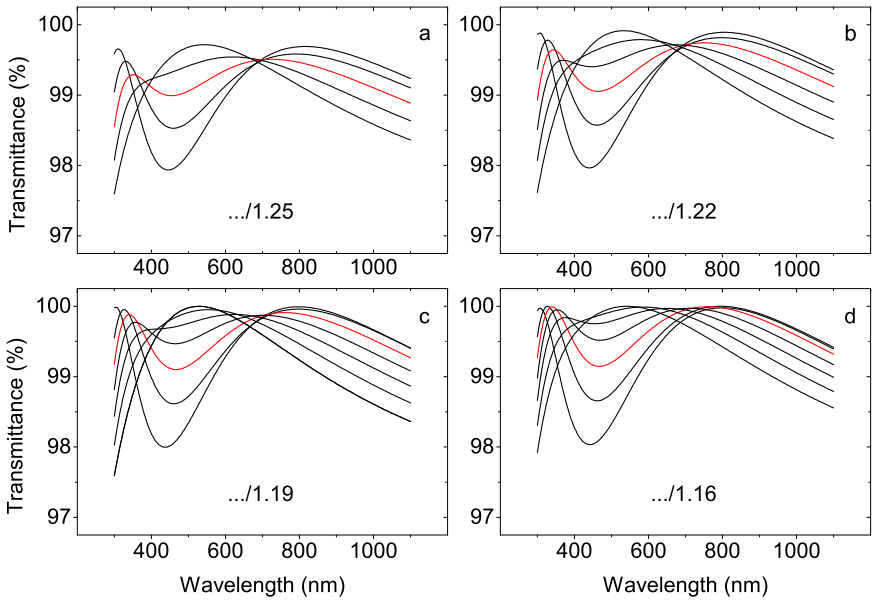

Fig. 3 Transmittance that changes with n_2 when n_1 is fixed. The curves go up with an increase of n_2 in the visible region, and the *red* lines represent the best results.

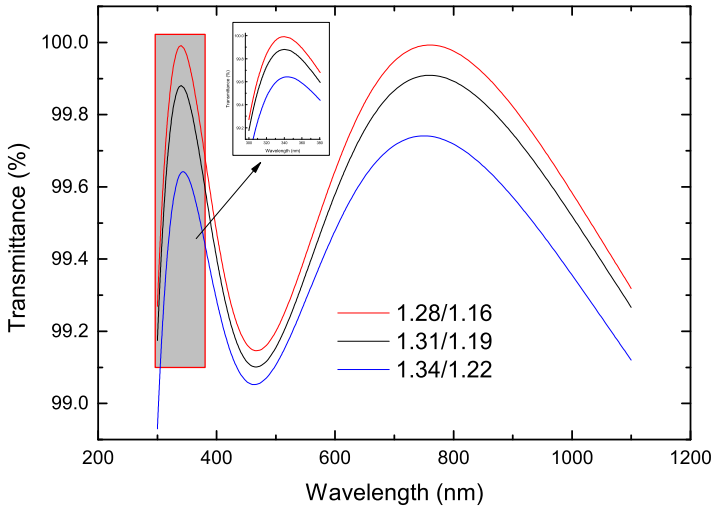

Fig. 4 Three best results from Fig. 3.

shown in Figure 2. In general, the curves decline with an increase of RI for the outer layer in the visible region; whereas, in the ultraviolet and near infrared regions, the condition is complicated in that the curve is crossed, which is not serious. Therefore, it can be approximated that the smaller the outer layer RI is, the higher the transmittance is. Except in Figure 2a, each figure has a unimodal curve (red lines) that appears to be different from others, which results when the outer layer RI is greater than that of the inner layer. The simulation results show that the outer layer thickness is zero, that is, the two-layer system degenerates into a single layer, so the inequality $n_1 < n_2$ must be implemented when applying two-layer AR coatings.

Then we fix n_1, that is, Sub/$\cdots$/n_1/Air. In view of the above conclusions drawn when n_2 was fixed, several RI combinations that have a small value of n_1 were chosen to be discussed, with the restricted condition $n_1 < n_2$, which is illustrated in Figure 3. It is obvious that the transmittance curves rise with an increase of RI

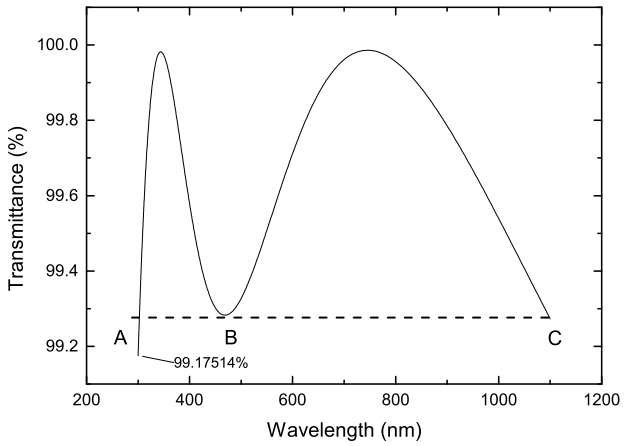

Fig. 5 The best result of the two-layer system, i.e. Sub/1.29/1.16/Air. A, B and C are three minimum points.

for the inner layer in the visible region, whereas, there is a converse variation in the ultraviolet and near infrared regions.

Among these different curves, we should choose the optimal one, which is dependent on the specific spectral requirements for transmittance, e.g., the requirement of high transmittance in a relatively narrow band, or that an average transmittance is as high as possible in the whole band, and there would be different optimization results with regard to various spectral performance requirements. Here, our optimization target is maximizing the lowest transmittance in the region from 300 nm to 1100 nm, that is, $\max\left(T_{\min}(\lambda)\right)$.

According to the optimization target, we choose three best results for n_2/n_1 from Figure 3b, c and d, respectively, namely, 1.34/1.22, 1.31/1.19 and 1.28/1.16 (Fig. 4). Apparently, the combination of 1.28/1.16 is the best. In order to make the results more accurate, we have RIs in the range $1.25-1.31$ discretized by $\Delta n = 0.01$; in view of practical feasibility, the lowest RI can be set as 1.16. With the same optimization method, we get the best result, 1.29/1.16, as shown in Figure 5. The minimum transmittance is $T_{\min} = 99.175\%$, which is the highest value we believe that could be theoretically achieved.

Figures 4 and 5 show curves in the shape of an "M" in the target waveband, which has a minimal value in the visible region, and two maximal values in the ultraviolet and near infrared regions. In the visible region, the curves meet the conditions $T \propto 1/n_1$ and $T \propto n_2$, but there is an opposite variation trend in the other wavebands, bounded by wavelengths at two maximal transmittances. In other words, the trend of the middle part of the "M" curve is opposite to that of the two sides. So, the process of seeking the optimal solution could be intuitively expressed as finding a curve that makes the minimum point equal to the edge transmittance on both sides of the band, that is, having the three points A, B and C on the same line but as far apart as possible (Fig. 5).

Since the sol-gel method is affected by many technological conditions it is impossible to precisely adjust the RI and film thickness during the actual fabrication. In the following part of this section, we will discuss the effect of small changes in the optical constant on the transmittance curve.

We take the best coating structure 1.29/1.16 for example. Several cases with $\Delta n = 0.01$ are shown in Figure 6. The small error of the RI makes a transmittance variation of about 0.1% in the short wave region, and 0.05% in the infrared region, which are acceptable.

It is well known that changes in the thickness of optical coating could lead to horizontal movement of the transmittance curve. We still choose the combination 1.29/1.16 to do our analysis, because the designed value of its physical thickness is d_1 =102 nm and d_2 =91 nm.

Figure 7 shows variation of transmittance with the film thickness error $\Delta d_1 = \pm 5$ nm. The average transmittance of the whole band remains unchanged, but the curve shifts to the infrared region as the thickness increases. As a result, the main variation of $T_{\min}$ occurs at the edges of the band, i.e., 300 nm and 1100 nm. There is a decline in transmittance of 0.3% at 300 nm when $\Delta d_1 = +5$ nm, yet only a decline of 0.1% at 1100 nm when $\Delta d_1 = -5$ nm. This is because the slope of the curve near 300 nm is larger than that near 1100 nm. As a consequence, there is a greater influence in the ultraviolet region, so we prefer the positive physical thickness errors supposing that the error exists. The inner layer shares a similar error rule with the outer layer. Another significant

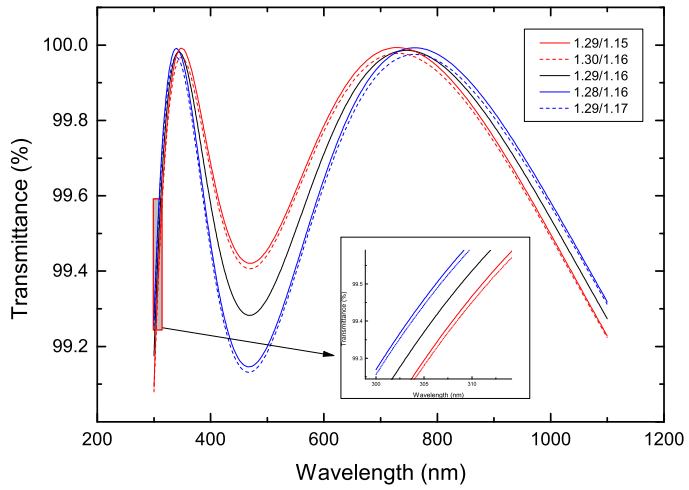

Fig. 6 Influence of minor error in RI on transmittance. The *black* line in the middle represents 1.19/1.16, the two *red* lines above share the same difference in RI of 0.14 and the two *blue* lines are 0.12.

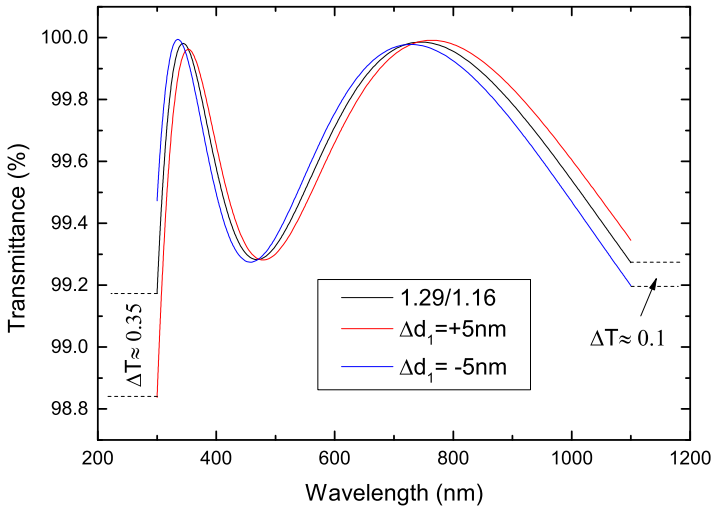

Fig. 7 Influence of film thickness error on transmittance. $\Delta d_1 = +5$ nm (*red* line) and $\Delta d_1 = -5$ nm (*blue* line).

practical guiding conclusion is that the thickness error of a single layer (which is as small as possible) does not affect the transmission curve if we keep the total thickness of the two layers constant. In the actual process of applying the coating, therefore, we can test the thickness after one layer is applied, and then eliminate the thickness error by adjusting subsequent layers.

Let us go back to Figure 6. The two clusters of curves on both sides of the optimal curve are almost coincident with no crossings, and similar features are also found in Figure 4 for a total of three clusters of curves. These three clusters of curves are characterized by a fixed RI difference between two layers. Then we draw a series of curves with an RI difference of 0.13, as shown in Figure 8. When n_1 and n_2 change by 0.03 simultaneously, $\Delta T \approx 0.1$. Compared with the results in Figure 6, we believe that the optimal RI difference between two layers is 0.13, and the more deviation there is from this value, the farther the transmittance deviates from the optimal solution. However, the synchronous RI errors from two layers will introduce less variation in transmittance than the individual error from one layer. Under the premise of maintaining Δn, the lower the RI of the outer layer is, the higher

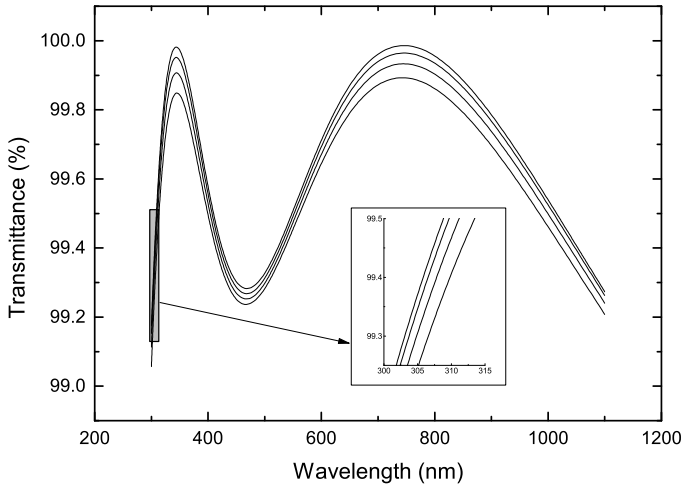

Fig. 8 A cluster of curves with an RI difference of 0.13. n_1 and n_2 change by 0.03 simultaneously.

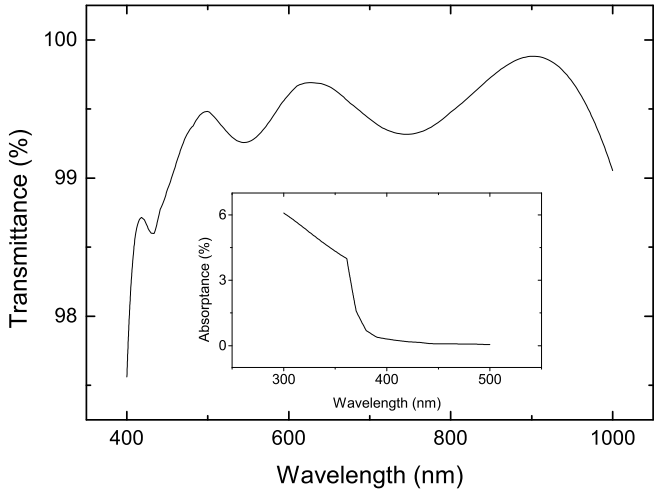

Fig. 9 The transmittance of single-side coated films in Table 1. The absorbance of quarter-wave TiO_2 coatings from 300 nm to 500 nm is shown in the inset.

Table 1 Parameters used to construct a typical 8-layer dielectric film stack with a substrate of fused silica. The reference wavelength is 510 nm.

Layer	Material	RI	Extinction coefficient	Optical thickness (FWOT)	Physical thickness (nm)
Medium	Air	1	0		
1	MgF_2	1.38542	0	0.28857433	106.23
2	TiO_2	2.34867	0.00037	0.09577107	20.8
3	SiO_2	1.4618	0	0.0612797	21.38
4	TiO_2	2.34867	0.00037	0.51796575	112.47
5	SiO_2	1.4618	0	0.04651835	16.23
6	TiO_2	2.34867	0.00037	0.1164711	25.29
7	SiO_2	1.4618	0	0.12799445	44.66
8	TiO_2	2.34867	0.00037	0.04589671	9.97
Substrate	SiO_2	1.4618	0		
Total				1.30047145	357.02

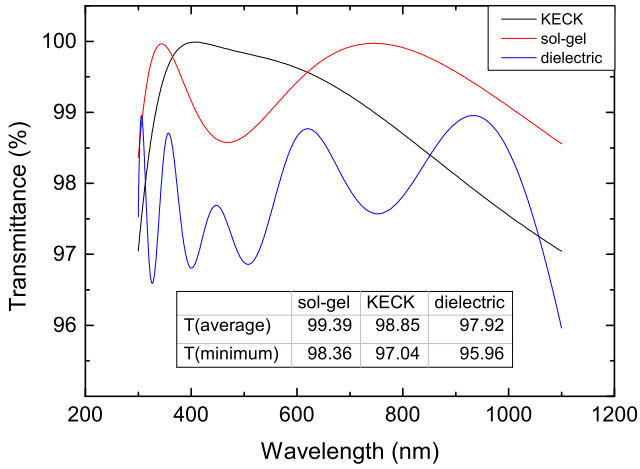

Fig. 10 The double-sided transmittance of 8-layer dielectric, KECK and sol-gel coatings as a function of wavelength from 300 nm to 1100 nm. The table in the inset lists statistical data on average and minimum transmittance.

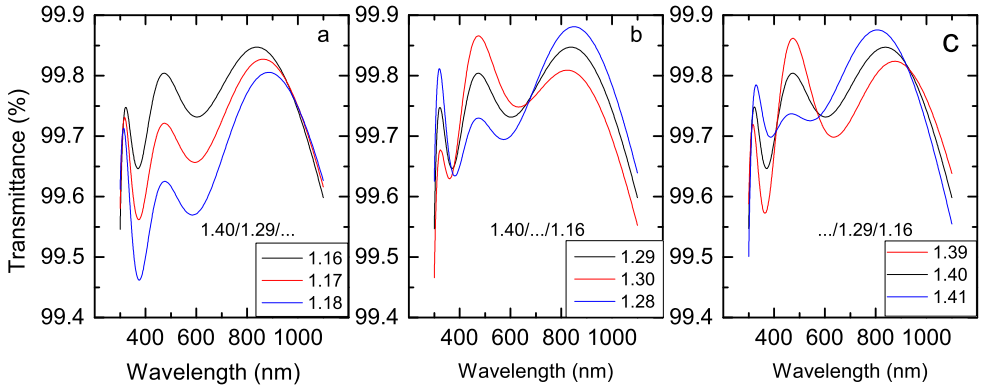

Fig. 11 Transmittance variation for different fixed RI of three-layer AR coatings.

the transmittance becomes. This conclusion is of great significance in guiding the actual process.

3.2 Comparison with Vacuum Dielectric Film

Due to good performance of the two-layer sol-gel coatings, we believe a better result can be produced by increasing the number of layers with different RIs. However, before introducing a three-layer structure, we will make a comparison between the vacuum dielectric coating and the sol-gel coating.

Parameters used to construct a typical 8-layer structure with a substrate of fused silica are listed in Table 1, and the transmittance curve is shown in Figure 9. As we can see, the curve greatly decreases near 400 nm, which is caused by absorption from the TiO_2 layer. If we extend the band to 300 nm, the absorption will be more severe (Fig. 9 inset). A number of conventional dielectric materials have absorption in the ultraviolet region, which makes the vacuum dielectric film greatly disadvantageous when applied to wideband AR coatings.

Here, the TiO_2 layers are replaced with HfO_2 that has no absorption in the ultraviolet region, and we get a better result (Fig. 10). However, there are big challenges in coating homogeneity, coating stress and controlling the process as the number of layers increases. Therefore, it is almost the best result for the vacuum dielectric coating. However for the KECK telescope, a combination of silica sol-gel over dielectric MgF_2 was used, which provides a better result than traditional vacuum dielectric multilayer coatings.

Figure 10 shows the double-sided transmittance of a vacuum 8-layer coating, the KECK coating and sol-gel coating from 300 nm to 1100 nm, and the associated

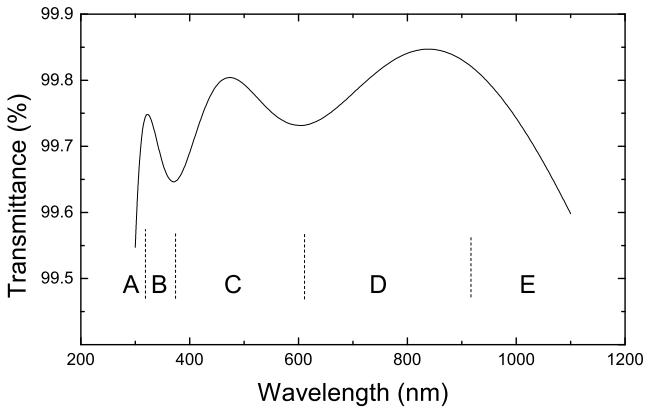

Fig. 12 The optimized curve for a three-layer coating, which uses 1.40/1.29/1.16.

Table 2 Variation rules for partition in Fig. 12

	A	B	C	D	E
$n_1 \uparrow$	↑		↓		↑
$n_2 \uparrow$	↓		↑	↓	
$n_3 \uparrow$	↓	↑	↓	↑	↓

statistical data are listed in the inset of Figure 10. Sol-gel coating has the highest average and minimum transmittance in the whole band, followed by KECK, and the worst is the dielectric coating, but there is a certain advantage in the visible waveband of the KECK coating. The reason why the KECK AR coatings have a somewhat poor result is that the MgF_2 layer has an RI of 1.37, far from the best n_2 (1.29). Therefore, it is possible to get a better result using the sol-gel two-layer structure than using the vacuum 8-layer or KECK coatings. The difficulty in achieving the theoretical value lies in the precise regulation of RI and thickness, which is the focus of the following experiment.

3.3 Three-layer System

The optimization methods are also applicable to three-layer structures. Firstly, we draw several curves to understand how transmittance changes with the RI of the three layers (Fig. 11), and then do a simple partition of it and give a summary of the variations in Table 2. From this rule, we can gradually adjust the curve for any combination of RIs until the target requirements are satisfied, that is, having the minimum points on the same horizontal line, as much as possible.

Figure 12 shows the optimized curve, which is 1.40/1.29/1.16, and $\Delta n \approx 0.12$. We also make a comparison between the two-layer and three-layer systems in Figure 13b. The two have approximately the same average transmittance (99.68% and 99.76% for the two-layer and three-layer cases, respectively), but the three-layer system possesses a better spectral reproduction ability and smaller fluctuations, with single-sided transmittance being more than 99.6% in the whole band.

In consideration of the experiences above, we may expect a better spectral performance with ever-increasing layers, however, the results are not notably better than the three-layer system after a large number of simulation tests. Moreover, difficulties in manufacturing increase rapidly with an increasing number of layers, so it is not practical. Let us go back to the simulations related to the two-layer and three-layer systems. The lowest RI is 1.16, and there is a big gap from the air, which limits the ultimate performance. In fact, the degree that transmittance performance might achieve is mainly determined by the outermost film, so we would expect a better result as n_1 is decreasing, as shown in Figure 13a.

Comparing the results of two-layer and three-layer structures, we found that the difference in RI from adjacent layers is about 0.11–0.13. Without considering the actual feasibility, the silica sol-gel on a fused silica substrate is no more than four layers. Figure 13b shows one of the results, with a minimum transmittance of 99.93% and an average transmittance of 99.98%, indicating an ideal approximately zero reflectance of no more than 0.07% in the whole band. This is a big gain in transmittance compared to the three-layer system. However, the most encouraging results stay in theory for now since

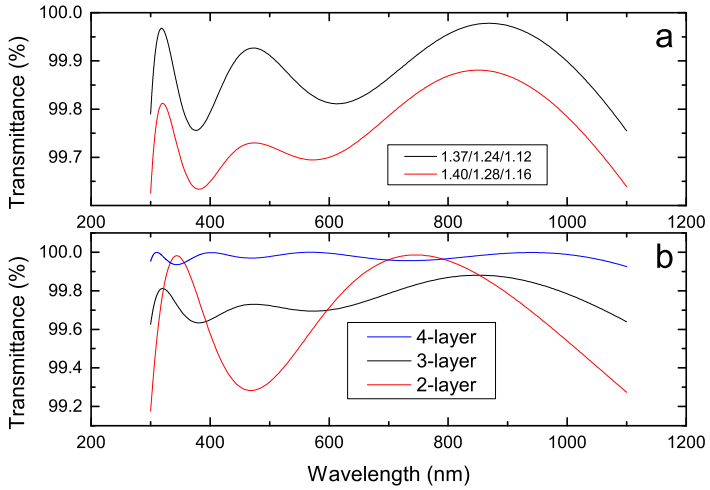

Fig. 13 (a) Comparison of three-layer coating with different n_1 which is available. (b) Optimum transmittance of 2-layer, 3-layer and 4-layer coatings.

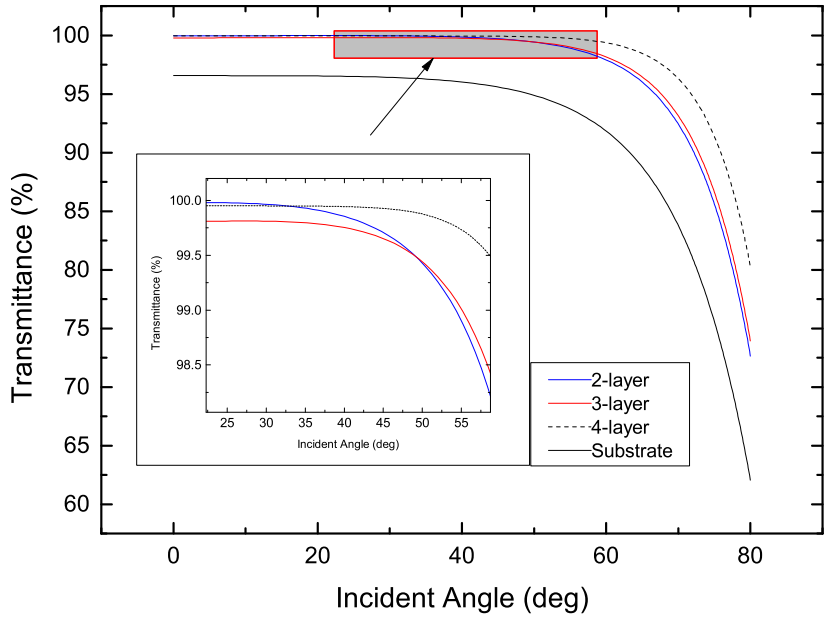

Fig. 14 Transmittance of bare substrate, 2-layer, 3-layer and 4-layer as a function of angle of incidence.

the sol-gel film, with an RI less than 1.1, is difficult to produce, and by reducing the outermost RI, a three-layer film could also yield a perfectly acceptable result. A comparison of two, three and four-layer coating single-sided transmittance is shown in Figure 13b.

Besides perfect broadband AR performance, the graded-index multilayer coatings also have great potential in suppressing reflection for a wide range of angles of incidence. The relationship between transmittance and angle of incidence for the two-layer, three-layer and four-layer sol-gel is shown in Figure 14. The curves corresponding to two and three layers are close to each other, and $T_{0-55} \geq 99\%$, $T_{0-72} \geq 90\%$. For the four-layer structure, $T_{0-62} \geq 99\%$, $T_{0-76} \geq 90\%$.

4 CONCLUSIONS

In this paper, we describe the structural designs for ultra-wideband AR coatings used in large aperture astronomical telescopes, and obtain the optimal solution by numer-

ical simulations. The error analysis and feasibility analysis are carried out according to the actual process of producing sol-gel which will provide abundant data that can support future experiments. In the end, we list several notes related to broadband multilayer coatings based on fused silica. The target band is 300–1100 nm.

(1) The RI of the coating gradually decreases from the substrate to the air, that is, $n_{\rm sub} > n_k > \cdots > n_1 > n_{\rm air}$, where k is the number of sublayers.
(2) The difference in RI between adjacent layers is about 0.11–1.13.
(3) On the premise of note 2, the lower the RI is of the outermost layer, the better the performance.

Satisfying the above conditions, silica sol-gel coatings are applied with a maximum of four layers, and the optical thickness of each layer is about one quarter of the reference wavelength. More layers cannot achieve remarkably better results. Taking into account practical feasibility, two or three layers can achieve a perfect result with an average transmittance of 99.7% in the region from 300 nm to 1100 nm.

The method used for our analysis is suitable for other bands and substrates. It is also instructive for large area AR coatings in the field of solar cells. Sol-gel films, due to their good broadband anti-reflection capability (especially in the ultraviolet band), simple manufacturing process, suitability for large area coating, high cost-performance ratio, etc, are believed to have prospects for wide application in the field of large aperture astronomical telescopes.

Acknowledgements This work was supported by the National Natural Science Foundation of China (Grant No. 11603055).

References

Anders, H., & Eichinger, R. 1965, Appl. Opt., 4, 899
Angeli, G. Z., Upton, R. S., Segurson, A., & Ellerbroek, B. L. 2004, in Proc. SPIE, 5382, Second Backaskog Workshop on Extremely Large Telescopes, eds. A. L. Ardeberg & T. Andersen, 337
Arnon, O. 1977, Appl. Opt., 16, 2147
Born, M., & Wolf, E. 1959, Principles of Optics Electromagnetic Theory of Propagation, Interference and Diffraction of Light (New York: Pergamon Press)
Dobrowolski, J. A., Poitras, D., Ma, P., Vakil, H., & Acree, M. 2002, Appl. Opt., 41, 3075
Huang, Y.-F., Chattopadhyay, S., Jen, Y.-J., et al. 2007, Nature Nanotechnology, 2, 770
Kanamori, Y., Ishimori, M., & Hane, K. 2002, IEEE Photonics Technology Letters, 14, 1064
Li, X., Gao, J., Xue, L., & Han, Y. 2010, Advanced Functional Materials, 20, 259
Liu, L.-Q., Wang, X.-L., Jing, M., et al. 2012, Advanced Materials, 24, 6318
Phillips, A. C., Miller, J., Brown, W., et al. 2008, in Proc. SPIE, 7018, Advanced Optical and Mechanical Technologies in Telescopes and Instrumentation, 70185A
Phillips, A. C., Miller, J., Cowley, D., & Wallace, V. 2006, in Proc. SPIE, 6269, Society of Photo-Optical Instrumentation Engineers (SPIE) Conference Series, 62691O
Rats, D., Poitras, D., Soro, J. M., Martinu, L., & Stebut, J. V. 1999, Surface & Coatings Technology, 111, 220
Ristau, D., Ehlers, H., Schlichting, S., & Lappschies, M. 2008, in Proc. SPIE, 7101, Advances in Optical Thin Films III, 71010C
Southwell, W. H. 1983, Optics Letters, 8, 584
Southwell, W. H. 1985, Appl. Opt., 24, 457
Tang, C. J., Jaing, C. C., Lee, K. H., & Lee, C. C. 2011, Applied Optics, 50, 62
Thomas, I. M. 1986, Appl. Opt., 25, 1481
Thomas, I. M. 1992, Appl. Opt., 31, 6145
Tokunaga, A. T. 2014, Chapter 51 - New Generation Ground-Based Optical/Infrared Telescopes (Elsevier Inc.), 413
Xi, J.-Q., Schubert, M. F., Kim, J. K., et al. 2007, Nature Photonics, 1, 176
Zhang, E.-P., Cui, X.-Q., Li, G.-P., et al. 2016, Research in Astronomy and Astrophysics, 16, 98